공학석사학위논문

Effect of 3D PEG Scaffold Hybridized with MC3T3-E1 Cell-derived Extracellular Matrix on Osteogenesis of Human Mesenchymal Stem Cell

MC3T3-E1 세포주 유래 세포외기질과 융합된
PEG 3차원 지지체의 골분화능

2018년 2월

서울대학교 대학원
화학생물공학부
김 슬 하

공학석사학위논문

Effect of 3D PEG Scaffold Hybridized with MC3T3-E1 Cell-derived Extracellular Matrix on Osteogenesis of Human Mesenchymal Stem Cell

MC3T3-E1 세포주 유래 세포외기질과 융합된
PEG 3차원 지지체의 골분화능

2018년 2월

서울대학교 대학원
화학생물공학부
김 슬 하

Abstract

Effect of 3D PEG Scaffold Hybridized with MC3T3-E1 Cell-derived Extracellular Matrix on Osteogenesis of Human Mesenchymal Stem Cell

Seulha Kim

School of Chemical and Biological Engineering

The Graduate School

Seoul National University

Existing studies about utilizing extracellular matrix (ECM) has focused on organs obtained from living organisms. But there is limitation in supply of organs has limited supply and the composition and therapeutic efficacy of ECMs has distribution depending on the factors represented as donor's health status and age. In contrast, the extracellular matrix obtained from the cell line cultured in the laboratory has the advantage; it could be produced under controlled environment with uniform quality. In this study, we developed an optimized decellularization process to separate the ECM of osteoblast cell line, MC3T3-E1. And we cultured human bone marrow-derived mesenchymal stem cells with the hydrolyzed ECM to evaluate bone-differentiation ability. Osteogenesis of the stem cell was analyzed by ALP staining, alizarin red S staining and real-time PCR. As

a result, we confirmed the statistically significant osteoinductivity of the ECM produced by MC3T3-E1 cell line in 2D and 3D condition. Our study suggests that ECM derived from cell lines could be utilized in tissue engineering fields as useful biomaterial.

Keywords : Osteogenesis, Mesenchymal stem cells, Extracellular matrix. Bone regeneration, Tissue engineering, PEG, scaffold

Student Number : 2016-21013

Contents

List of tables and figures

Introduction

The extracellular matrix (ECM) is complicated complex surrounding the cells, composed of secreted proteins, polysaccharides, growth factors and cytokine [1]. Recently, it has been found that the ECM has different composition depending on which organ or tissue it is derived from. ECM has decisive effect on cell's adhesion, proliferation, migration and differentiation through the interaction between ligands of ECM and cell's receptors [2]. Lots of the studies are going on to utilize ECM in tissue engineering [1, 3].

Existing researches have focused on the ECM obtained from organ of human, bovine or porcine. The process of removing cells and leaving only ECM from real tissue is called as decellularization. The actual organs of the organisms have a specific composition and structure that is mingled with other tissues such as fat or blood vessels, not just the target tissue. Decellularization process includes various treatments such as acid, base, enzyme, surfactant, and heat to obtain only the target ECM [4]. As mentioned above, the composition of ECM varies depending on the organ or tissue, appropriate decellularization process should be designed according to and the purpose tissue type.

The demineralized bone matrix (DBM) is a substance that removes cellular components and minerals from the actual bone and leaves only the bone ECM. DBM contains various important component of actual bone: bone-specific proteins and inorganic phosphate. It is a commercialized biomaterial which has both osteoconductivity and osteoinductivity. Long-term clinical results

demonstrate that this material promotes bone regeneration and fuses well with surrounding bone tissue. It has been used in various forms such as bone cement, putty and sponge [5, 6].

Although the demand for human bone-derived DBM is increasing for patients with bone defects, the supply of human bone tissue is limited. And DBM shows different clinical performance depending on the tissue donor's age and state of health [7, 8]. Biomaterials utilizing decellularized organ, including DBM, can be costly and time consuming because sufficient inspection and sterilization process are required in case transplant carry a deadly infectious diseases such as Creutzfeldt-Jakob disease, SARS or AIDS [9, 10].

These disadvantages have led to the development of inorganic materials that can be produced at uniform quality in factories such as mineralized xenografts, hydroxyapatite, and polymers to replace DBM, but the therapeutic effect is not sufficient to be used as a substitute for DBM [11].

To solve this problem, we focused on the ECM produced from *in vitro* cultured cell line. The ECM derived from the cell line can be obtained in uniform and controlled condition. Also the process of removing cells and minerals, and sterilizing is much easier and faster than the actual bone. Because the ECM produced by the cell line is obtained in the form of a thin sheet that can be easily separated, produced in a sterile environment, and grown without unnecessary tissue such as blood vessels and fats. The decellularization step proceeding in mild conditions is expected to reduce the loss of important functional agent.

The MC3T3-E1 cell line used in this study is a preosteoblast cell line obtained from the mouse calvaria, which rapidly proliferates and secretes a large amount of collagen-based ECM after differentiation [12, 13]. We established a decellularization protocol to remove the cells by simple chemical treatment and evaluated that the cell components were sufficiently removed through our process by DAPI staining. After this process, the separated ECM was hydrolyzed using pepsin, and osteoinductivity of the digested ECM was confirmed using human bone marrow-derived mesenchymal stem cells. Stem cells were induced bone differentiation in 2D: cultured on the digested ECM coated dish, and in 3D: cultured on the ECM hybrid scaffold.

The base material of the scaffold is poly (ethylene glycol) diacrylate (PEGDA). PEG is a synthetic polymer that is hydrophilic and stable in the body. so it is attracting attention as a biocompatible and bioinert material [14, 15]. In this study, we manufactured PEG scaffolds fused with digested ECMs to confirm the efficacy of digested ECM in three dimensions.

Materials & methods

1. Cell culture: MC3T3-E1

MC3T3-E1 subclone 4 was purchased from the American Type Culture Collection (ATCC, cat. CRL-2593) and cultured following supplier's protocol. Cells were maintained in Alpha Minimum Essential Medium (αMEM; Gibco, cat. A1049001) without ascorbic acid. This basal medium was supplemented with 10% fetal bovine serum (FBS; Biowest, cat. S1520), 50 units/ml penicillin and 50 μg/mL streptomycin (Gibco, cat. 15140-122). Cells were transferred to a fresh flask via 0.25% Trypsin-EDTA (TE; Gibco, cat. 25200-056) when they reached 90% cellular confluence. Medium was exchanged every 3 days. To produce extracellular matrix (ECM), 10^5 cells were seeded on a 75 cm^2 flask. And the medium for cell culture including 50 μg/ml ascorbic acid and 10 mM β-glycerophosphate disodium salt hydrate (Sigma, cat. G9422) were utilized for ECM production. MC3T3-E1 cells were cultured without transfer for 14 days to produce thick ECM layer. The cells were incubated in humidified 37℃ and 5% CO_2 (Panasonic, cat. MCO-20AIC-PK).

2. Decellularization

The layer of ECM with cell could be easily detached from cell culture dish by gentle pipetting or dish shaking. Detached ECM with cell layer was treated with TE for 60 sec followed by 10 sec vortex in double distilled water (DDW). After washed by phosphate buffered saline (PBS; Welgene, cat. LB 204-02), the ECM was

treated with 0.1% TritonX-100 in PBS (PBST) for 30 minutes to remove the remaining cells. Then, ECM layer was washed with PBS repetitively and stored in PBS at -20℃ (fig. 1.1).

3. DAPI staining

Cells or scaffolds were washed with PBS for several times and had fixed with 4% paraformaldehyde (PFA; Biosesang, cat. P2031) for 5 minutes. After that, samples were washed twice with PBS. 300 nM DAPI (Invitrogen, cat. D1306) solution was added to the sample for 5 minutes in the dark. After washing more than 3 times with PBS, the blue fluorescence was observed under fluorescent microscope (Olympus, cat. IX71), All of the steps were conducted at room temperature.

4. ECM Digestion

Decellularized ECM was digested by modified Freytes' protocol [16] for the ECM application. Briefly, after lyophilization and chopping, 1 g ECM was mixed with 100 mg pepsin from porcine gastric mucosa (Sigma, cat. P7012) and 0.01 M 100 ml HCl in PBS. ECM went through enzymatic hydrolysis for 6 hours at 25~30℃ (fig. 1.2 (a)). 0.1M NaOH was added to deactivate the pepsin. After that, ECM sheet was torn into small pieces on the scale of several hundred micrometers (fig. 1.2 (b)). Digested ECM was stored at -20℃ until used.

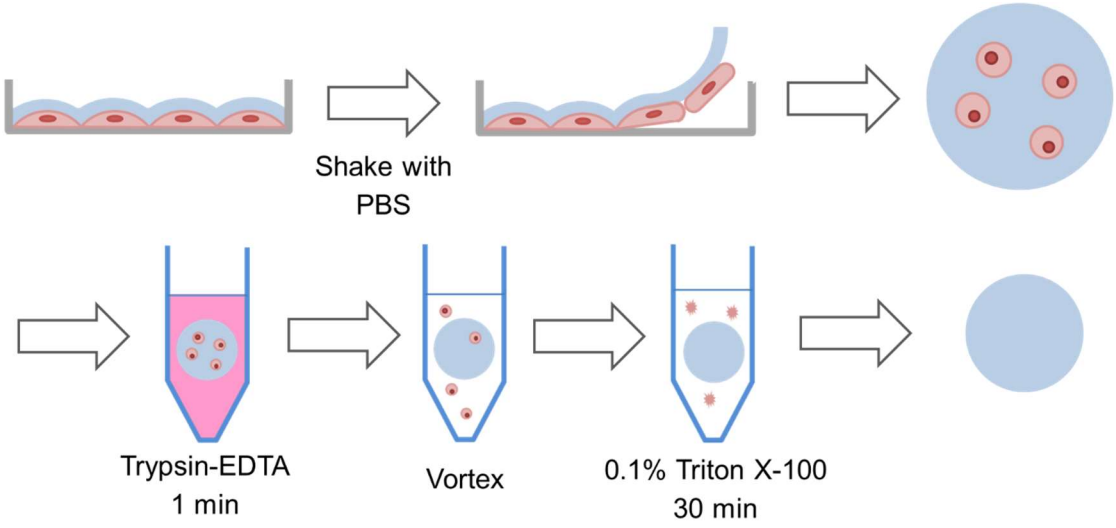

Figure 1.1 Schematic image of decellularization process. Light pink and red circles means cells and nuclei, each. Light sky color means ECM produced by cell line.

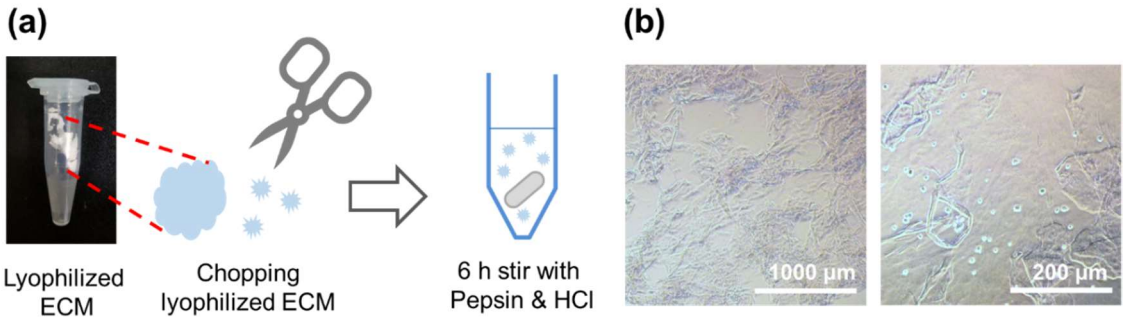

Figure 1.2 Digestion of harvested ECM. (a) Schematic image of ECM digestion process. Digestion solution was mixed with a magnetic stirring bar (light gray oval) during the reaction. (b) Optical images of digested ECM pieces observed in bright field.

5. Coating

To confirm osteoinductivity of digested ECM in 2D, the ECM was coated on the 24 well plate. As control group, rat tail derived collagen type I (BD bioscience, cat. 354236) was coated on the 24 well plate. Each well was coated with 400 ng/100 μl of the digested ECM or the collagen type I with PBS at pH 7 and incubated at 37℃ for 30 minutes.

6. Scaffold preparation

We prepared ECM-hybrid scaffold using polyethylene glycol diacrylate, M.W. 3400 (PEGDA; Alfa Aesar, cat. 46497) via modified procedure [17]. Each concentration of PEGDA, ammonium persulfate (APS; Sigma, cat. A3678) and N,N,N,N-tetramethyl-ethylenediamine (TEMED; Sigma, cat. T9281) was same for all groups: 9.5%, 0.5% and 0.25%, respectively. Only digested ECM concentration was changed (table 1.1). All of the reactants were dissolved in PBS at 4℃, and then the mixture was polymerized overnight at -20℃ (fig. 1.3). Two different size scaffolds were produced; small size scaffold was made using 20 μl volume mold (diameter 5 mm, height 1 mm) and large size scaffold was made using 200 μl volume mold (diameter 10 mm, height 3 mm). After lyophilization, the scaffolds were sterilized via UV for 2 hours at room temperature. Then the scaffolds were washed with PBS to remove unreacted chemicals before cells seeding. Small size scaffolds were used for the cell culture and large size scaffolds were used for measurement of mechanical properties.

Group	Control	I	II	III	IV	V
PEGDA (w/v)	9.5%	9.5%	9.5%	9.5%	9.5%	9.5%
APS (w/v)	0.5%	0.5%	0.5%	0.5%	0.5%	0.5%
TEMED (v/v)	0.5%	0.5%	0.5%	0.5%	0.5%	0.5%
Digested ECM solution (v/v)	0%	12%	24%	36%	48%	60%

Table 1.1 The proportion of protein and other constituents in ECM-hybrid PEGDA scaffold preparation. From control group to group V, digested ECM solution content increased with constant rate.

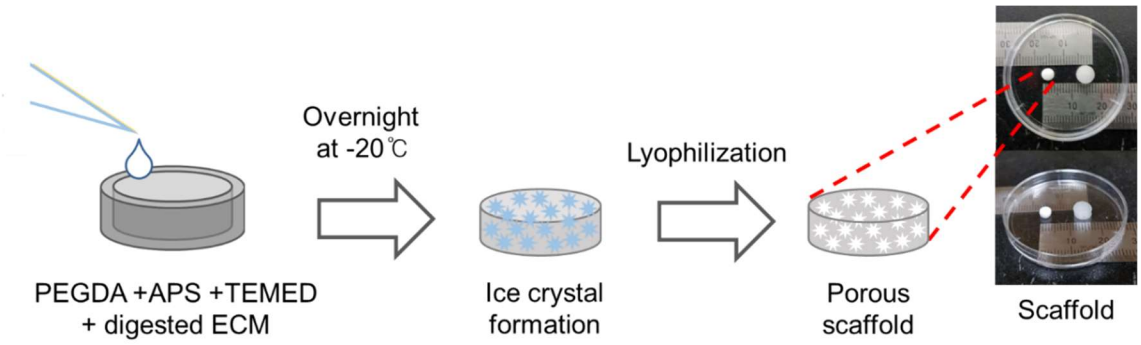

Figure 1.3 Schematic image of manufacturing ECM-hybrid PEGDA scaffold. Ice crystals were formed between polymer and constructed porous structure.

7. Cell culture: hMSC

Human bone marrow-derived mesenchymal stem cells (hMSCs) were purchased from Lonza (cat. PT-2501, 23 years old, black, female) at passage 2. hMSCs were maintained following the company's protocols. Briefly, the cells were grown in MSCGM (Lonza, cat. PT-3001) 100 μg/ml primocin (Invivogen, cat. ant-pm-1) and transferred via TE. Cells in passage 5 to 7 were used for experiment. We seeded 10^4 cells per well of 24 well plate, and $5x10^4$ cells per the small size scaffold.

Osteogenic medium was Dulbecco's Modified Eagle's Medium high glucose (DMEM; Biowest, cat. L0103-500) supplemented with 10% FBS, 50 units/ml penicillin, 50 μg/mL streptomycin, 100 μg/ml primocin, 100 nM dexamethasone, 50 μM ascorbic acid and 10 mM β-glycerophosphate. The cells were cultured in humidified 37℃ incubator with 5% CO_2. Medium was exchanged every 3 days.

8. Scaffold characterization

After that, the surface of scaffold's morphology and mechanical properties were measured in large size scaffold. After lyophilization, samples were coated with platinum at 20 mA for 100 sec. Manufactured large size scaffold was observed via field emission scanning electron microscopy (FE-SEM; JEOL, cat. JSM-6701F).

To measure the swelling ratio of large size scaffold, lyophilized scaffolds were induced to equilibrium state in DDW for 5 min. After removing the excess water below, swelling ratio was calculated as following equation. W_{wet} means weight of scaffold absorbed sufficient water and W_{dry} means weight of lyophilized scaffold.

$$\text{Swelling ratio} = \frac{W_{wet} - W_{dry}}{W_{dry}} \times 100\ (\%)$$

Young's modulus of the scaffold was also measured in wet state. The change of the compressive force along the change of length was measured by tensile tester (Shimadzu, cat. EZ-SX) and the young's modulus value was obtained from the slope at the initial section of the graph.

9. Alizarin red S staining

Cells were stained with Alizarin Red S (ARS; Sigma, cat. A5533) to see the mineral crystals produced by differentiated mesenchymal stem cells. After filtering through 0.45 μm pore size filter, 2% (w/v) ARS solution in DDW was treated to the 4% PFA fixed cells. Samples were washed with DDW between every step and all the process was conducted at room temperature.

To quantify the amount of deposited minerals, cetylpyridinium chloride (Sigma, cat. C0732) was used. After dissolving the ARS via cetylpyridinium chloride 10% (w/v) in DDW for 30 minutes. The absorbance of the solution was measured at 545 nm by microplate reader (TECAN, cat. SPARK 10M).

10. F-actin staining & Immunostaining

F-actin of hMSCs was stained with alexa fluor 488 dye attached phalloidin (Invitrogen, cat. A12379). Staining procedure was modified from manufacturer's recommended procedure. Scaffolds were fixed in 4% PFA for 10 min. And cells were permeabilized via 0.1% PBST for 10 min. For blocking, cells were incubated

with 1% BSA in PBS for 30 min. The cells were then stained via 5 units/ml of phalloidin with alexa 488 in PBS for 40 min. All of the steps were conducted at room temperature.

For the detection of the ECM fragments, primary antibody for collagen type I (Abcam, cat. ab34710, dilution 1/500) was applied for overnight at 4℃. Sequentially, anti-rabbit antibody (Invitrogen, cat. A11012, dilution 1/40) was applied for 1 h at room temperature. DAPI staining was conducted in the same way as mentioned above. Samples were washed with PBS between every step. Then, samples were observed via confocal laser scanning microscope (CLSM; Carl Zeiss, cat. LSM710).

11. CCK-8 assay (proliferation assay)

Effect of scaffolds on hMSCs' proliferation was evaluated by cell counting kit-8 (CCK-8; Dojindo, cat. CK04-11) assay following the manufacturer's instructions. Initially, 50000 cells were seeded on each scaffold. To remove the non-attaching cells, medium (MSCGM) was completely exchanged after 24 h. After incubation with 10% (v/v) CCK-8 in medium for 3 h in a humidified 37℃, 5% CO_2 condition, the absorbance of the supernatant was measured with microplate reader (TECAN, cat. SPARK 10M) at 450 nm. CCK-8 assay was conducted after 2, 10 and 20 days.

Results

1. Decellularization & digestion

When MC3T3-E1 cells were cultured with ascorbic acid, ECM complex with the cells was produced. Unlike real bones obtained from animal or human, ECM with cell has a form of thin, flexible sheets and do not contain other tissues such as fat (data were not shown). We created a protocol using TE and Triton X-100 to separate only the ECM from the complex.

To verify the effect of the decellularization method, we stained nucleus whether the cells were removed. As a result, it was confirmed that most of the cells were removed through the loss of blue-stained nuclei. Before decellularization, the nuclei were sporadically located on the ECM sheet (fig. 2.1 A). However, after the decellularization process, the blue fluorescence remarkably disappeared (fig. 2.1 B). Therefore, we decided to use this method to extract ECM through our overall study.

ECM was digested by pepsin before used in coating or preparation of the scaffold to manipulate with pipette and mix with polymer reagents. The ECM solution turned into a cloudy suspension and disintegrated enough to manipulate with pipette (fig. 1.2).

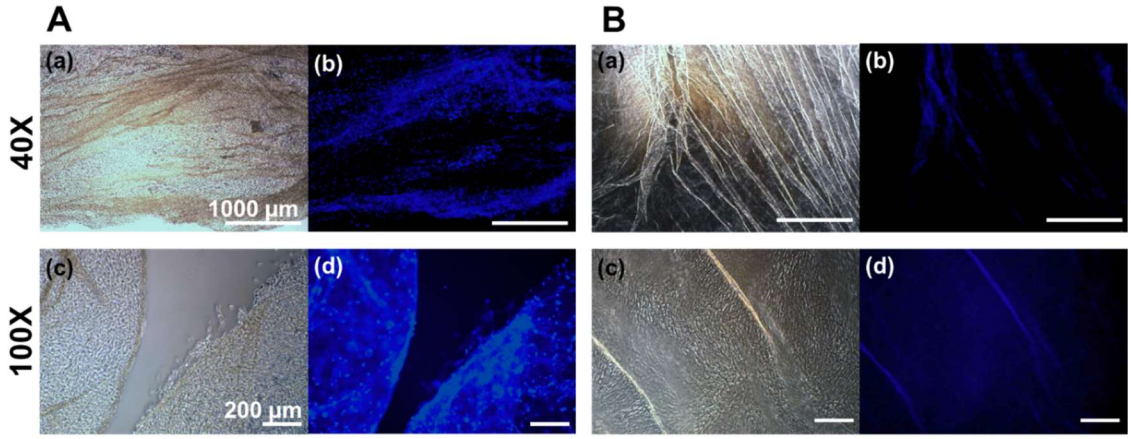

Figure 2.1 Evaluation of decellularization process by DAPI staining. Nuclei were stained with blue color using DAPI. A Bright field images (a), (c) and blue fluorescence images (b), (d) of the ECM-cell sheet before the decellularization. B Bright field images (a), (c) and blue fluorescence images (b), (d) of the ECM-cell sheet after the decellularization.

2. Osteoinductivity of digested ECM

To identify that digested ECM still preserving osteoinductivity, we coated digested ECM on the cell culture dish. It is well known that main component (>90%) of ECM produced by mature osteoblast is collagen type I. Non-coated cell cultured dish and collagen type I coated dish were also prepared as a control group. hMSCs were cultured on the coated dish for 10 and 20 days in osteogenic medium.

Early osteogenesis of hMSCs cultured on the coated dishes was identified with ALP staining. ALP staining kit (sigma, cat. 85L-2) measures alkaline phosphatase (ALP)'s activity through the appearance of purple as the reaction of the enzyme occurs. At 10 days, non-coated group and digested ECM coated group showed similar ALP activity (fig. 3.1 (a), (c)). Collagen coated group showed less purple color. In non-coated group and collagen coated group after 20 days, stained purple color was getting more intense (fig. 3.1 (d), (e)). But in the digested ECM group, purple color almost disappeared. The black arrows indicate ECM fragments and the purple color was not originated from the stained cells but ECM fragments (fig. 3.1 (f)).

We also stained hMSCs with Alizarin red S after 20 days to analyze mineralization ability of hMSCs differentiated into mature osteoblast state. ARS staining stains mineral crystals deposited in the ECM with red color. The more minerals were stained from non-coated to collagen type I and digested ECM coated group (fig. 3.2 (a) ~ (c)). Non-coated group was not stained at all (fig. 3.2 (a)). In the collagen

coated group, light orange dyed spots appeared and at the digested ECM group it was stained with a clear red color (fig. 3.2 (b), (c)). The black arrows point to the ECM fragments. ARS stained around these ECM fragments. By comparing fig. 3.2 (c) and (d), this clear red staining result was not reproduced when cells were cultured in non-osteogenic medium.

The amount of deposited minerals was quantified by cetylpyridinium chloride assay (fig. 3.3). Absorbance was measured at 540 nm and normalized by mean value of non-coated group. The digested ECM coated group showed significantly higher mineralization level (p value < 0.005). The graph revealed that digested ECM coated group deposited minerals about 6 times more than the collagen I coated group.

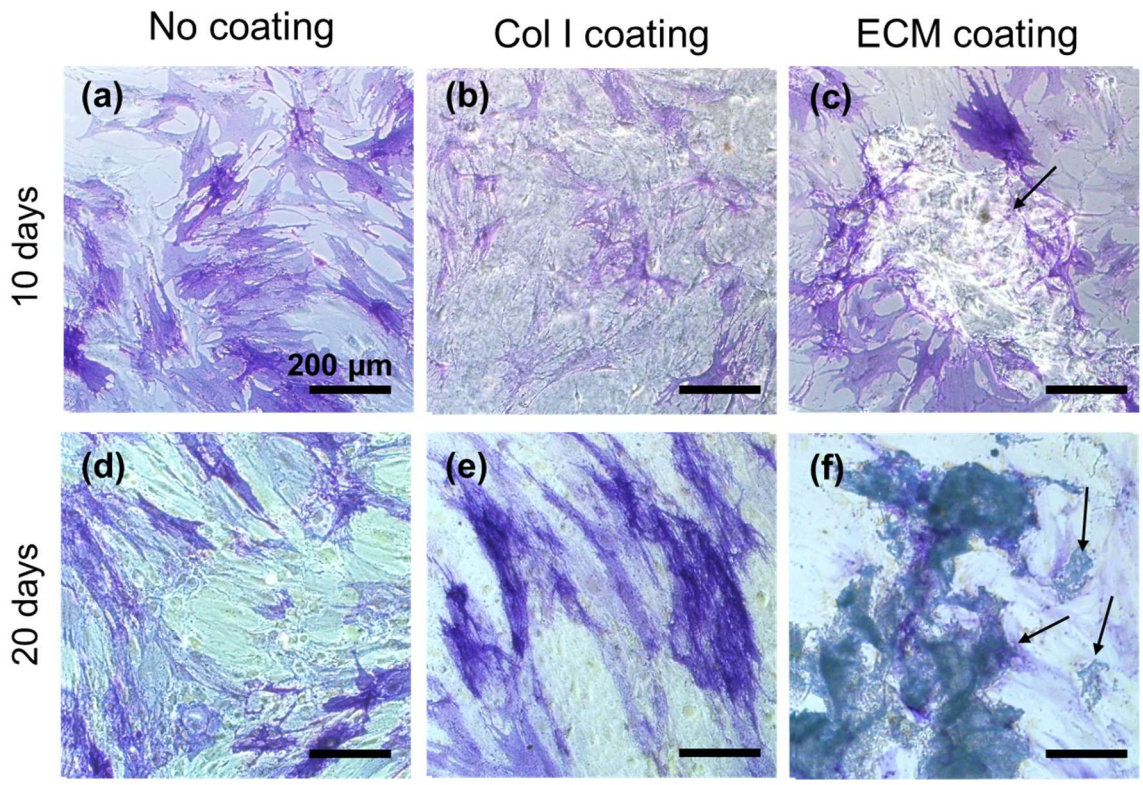

Figure 3.1 ALP Staining results of hMSCs cultured in 2D with osteogenic medium. ALP were stained as dark blue or purple. **(a) ~ (c)** Cells were stained after 10 days, and **(d) ~ (f)** after 20 days. Black arrows indicate digested ECM pieces.

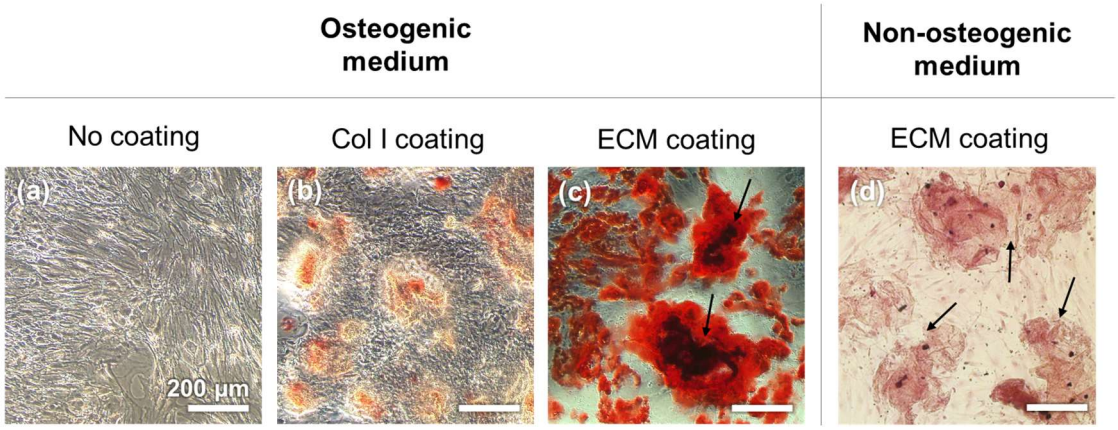

Figure 3.2 Analyzing mineralization of hMSC. ARS Staining results of hMSCs cultured in 2D. **(a) ~ (c)** Alizarin red S staining results after 20 days in osteogenic medium. **(d)** ARS staining results after 20 days in non-osteogenic medium. Minerals were stained as red. Black arrows indicate digested ECM pieces.

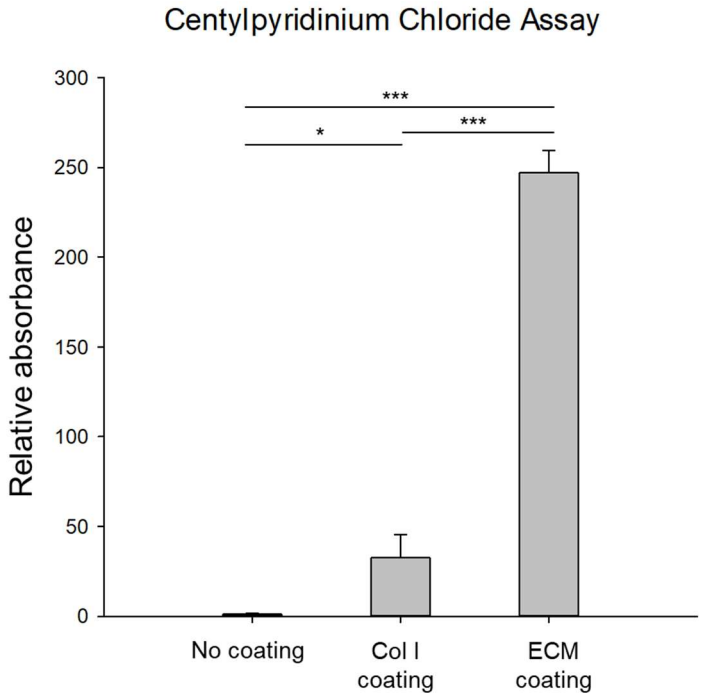

Figure 3.3 Quantification of deposited mineral via cetylpyridinium chloride assay. (n=4, * = $p<0.05$, *** = $p<0.005$)

3. Physical characterization of scaffolds

The scaffolds were manufactured in six groups that contained the same proportions of PEGDA, APS and TEMED, whereas the ECM concentration was different. The digested ECM solution percentage was linearly increased as group number and control group scaffold didn't include any ECM (fig. 4.1 (a)).

We observed cryogels via SEM to characterize its structure (fig. 4.1 (b)). From control to the group II, porous structures were well maintained. Group III and IV showed rough surface but still had uniform pore size. However, group V, the highest ECM content group, showed completely collapsed structure and detail porous structures were totally destroyed. With this result, we excluded group V from the rest experiment.

We measured swelling ratio of all groups (fig. 4.2). In group I ~ IV, they showed slightly irregular shape after swollen up (fig. 4.2 (a)), but swelling ratio was not far behind compared with control group (fig. 4.2 (b)).

Young's modulus represents the magnitude of force that can induce the same length change in the same cross-sectional area. The results from Young's modulus showed that group I~ IV had stronger mechanical property than control group (fig. 4.3). Young's modulus of ECM-hybrid PEG scaffolds was not far degraded, even increased when compared with control group.

(a)

Group	Control	I	II	III	IV	V
Digested ECM solution ratio	0%	12%	24%	36%	48%	60%

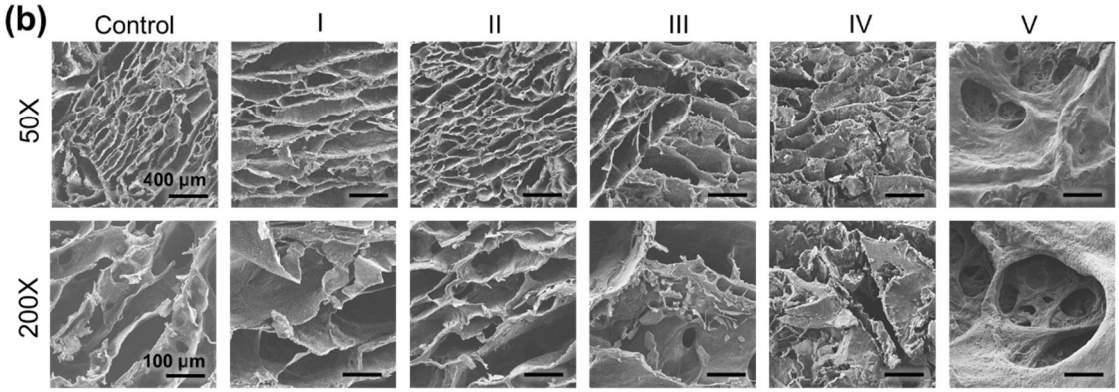

Figure 4.1 SEM images of ECM-hybrid PEGDA scaffolds. **(a)** Digested ECM solution content in each group of the scaffolds. The ratio of digested ECM solution increased according to the group numbers. **(b)** SEM images of the all scaffolds groups. Porous structure of the scaffolds was observed in 50x and 200x magnifications.

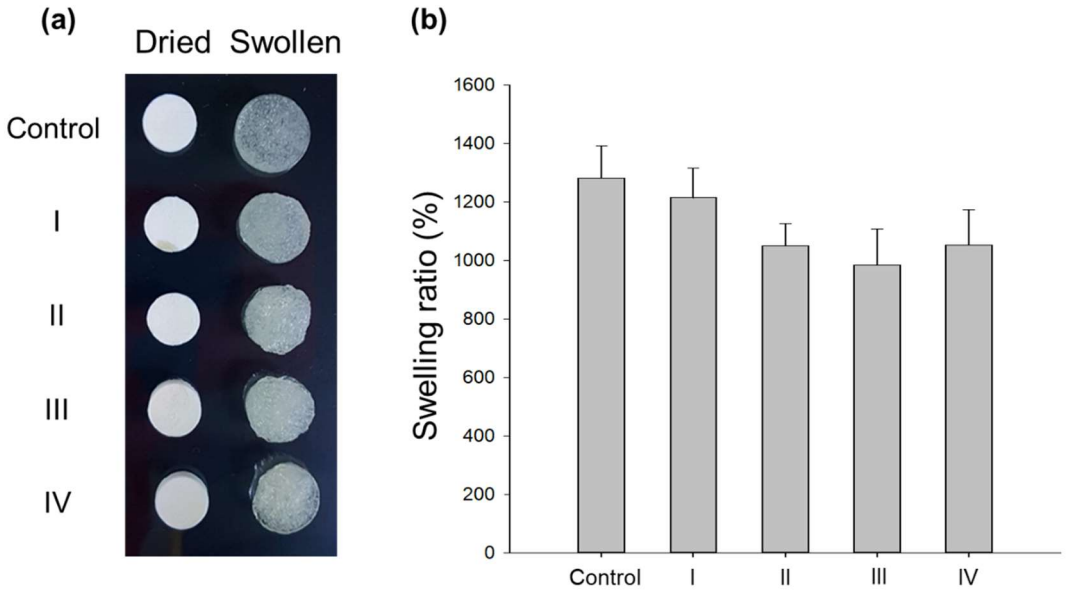

Figure 4.2 Measurement of swelling ratio. **(a)** Pictures of the large size scaffolds in dried and wet condition. **(b)** Weight swelling ratio of the scaffolds. (n=5)

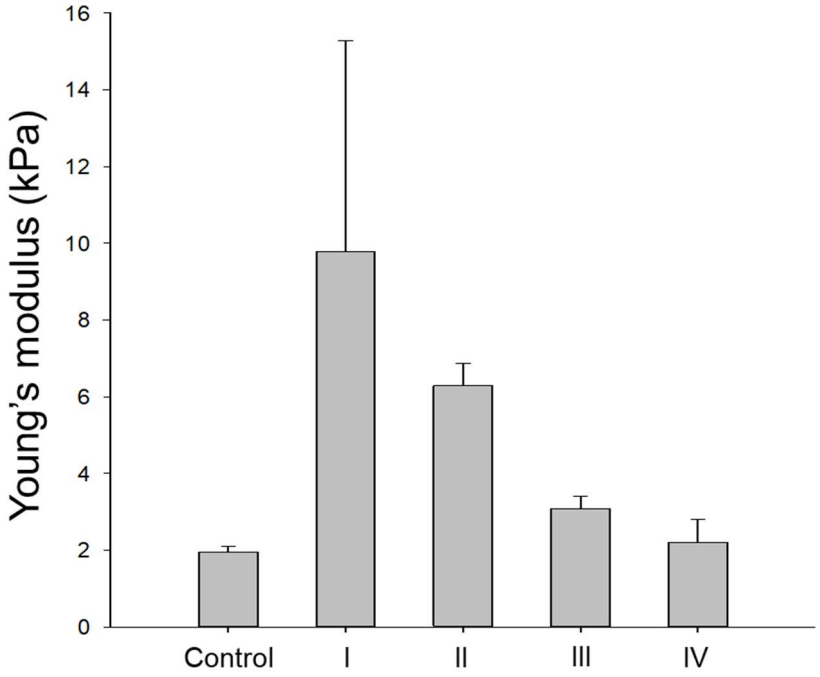

Figure 4.3 Calculation of Young's modulus. Modulus of the large size scaffold was measured in wet condition. (n=4)

4. Cell adhesion and proliferation in 3D

hMSCs were cultured with 3 scaffold groups: group IV including the highest ECM concentration, group II having half concentration, and control group. The effect of scaffold on early cell adhesion and proliferation rate was analyzed. Unattached cells were removed after 1 day from seeded. and stained with fluorescence dye after another 1 day. The nucleus, F-actin, and collagen type I were observed using a confocal microscope.

In the control group, the cells attached to the scaffold in the form of the cell aggregate, and did not stretched along the scaffold structure (fig. 5.1 (a) ~ (c)). In the enlarged image of the three-dimensional observation through the z-stack, the cells form a small spheroid (fig. 5.1 (d) ~ (f)).

In group II, though cell aggregates were still present, cells were attached with long stretches on the ECM fragment (fig. 5.2). In group IV, cells are all attached to the ECM fragment. Comparing the red fluorescence of the collagen type I originated from ECM fragment with the F-actin showing the area of the cells attached, excess surface of the ECM fragments remaining without the cells of the group IV was much larger than that of the group II (fig. 5.2, 5.3).

Fig. 5.4 is the image of the cells cultured on the control group scaffold after 10 days. Cell's F-actin shows extended shape. But nucleus distribution showed that cells formed dense cell assembly in the small size region (fig. 5.4 (d) ~ (f)).

We compared the proliferation rate of cells using the CCK-8 assay kit. Cells were seeded and unattached cells were removed after 1 day, so the absorbance

measured on day 2 corresponds to the initial cell adhesion. This result is consistent with what we have seen in fig. 5.1 ~ 5.3 After 10 and 20 days, cells proliferated in all three groups. The slope indicating the growth rate of cells was the fastest in the control group and slowest in group IV (fig. 5.5 (b)).

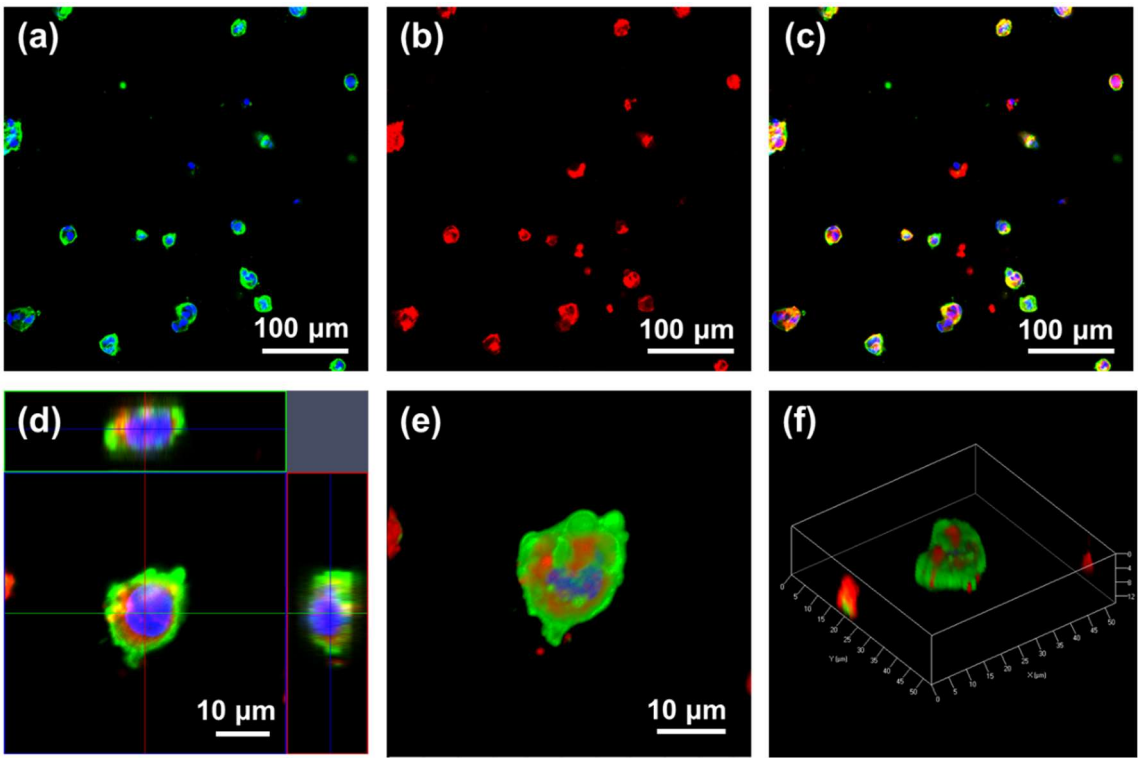

Figure 5.1 Immunofluorescence images of early cell adhesion on the control group scaffold. hMSCs were stained after cultured with osteogenic medium for 2 days. (Blue = nucleus, green = F-actin, red = collagen type I)

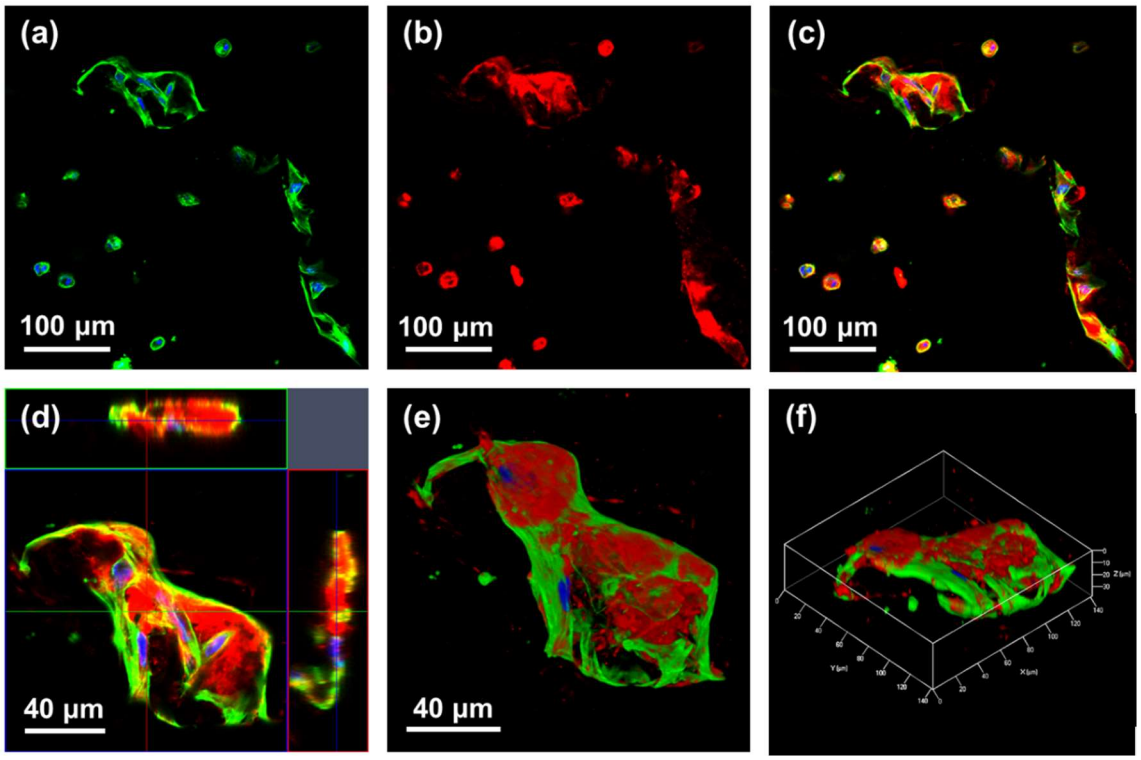

Figure 5.2 Immunofluorescence images of early cell adhesion on the group II scaffold. hMSCs were stained after cultured with osteogenic medium for 2 days. (Blue = nucleus, green = F-actin, red = collagen type I)

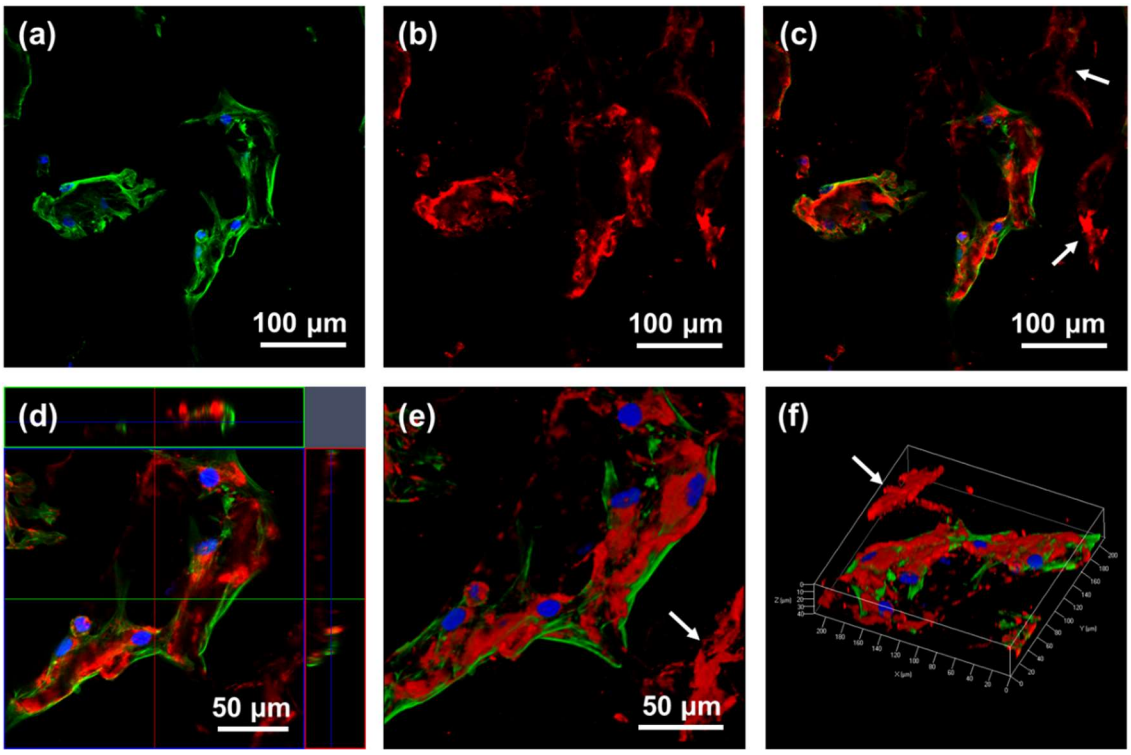

Figure 5.3 Immunofluorescence images of early cell adhesion on the group IV scaffold. hMSCs were stained after cultured with osteogenic medium for 2 days. White arrows indicate ECM fragment that cells were not attached.. (Blue = nucleus, green = F-actin, red = collagen type I)

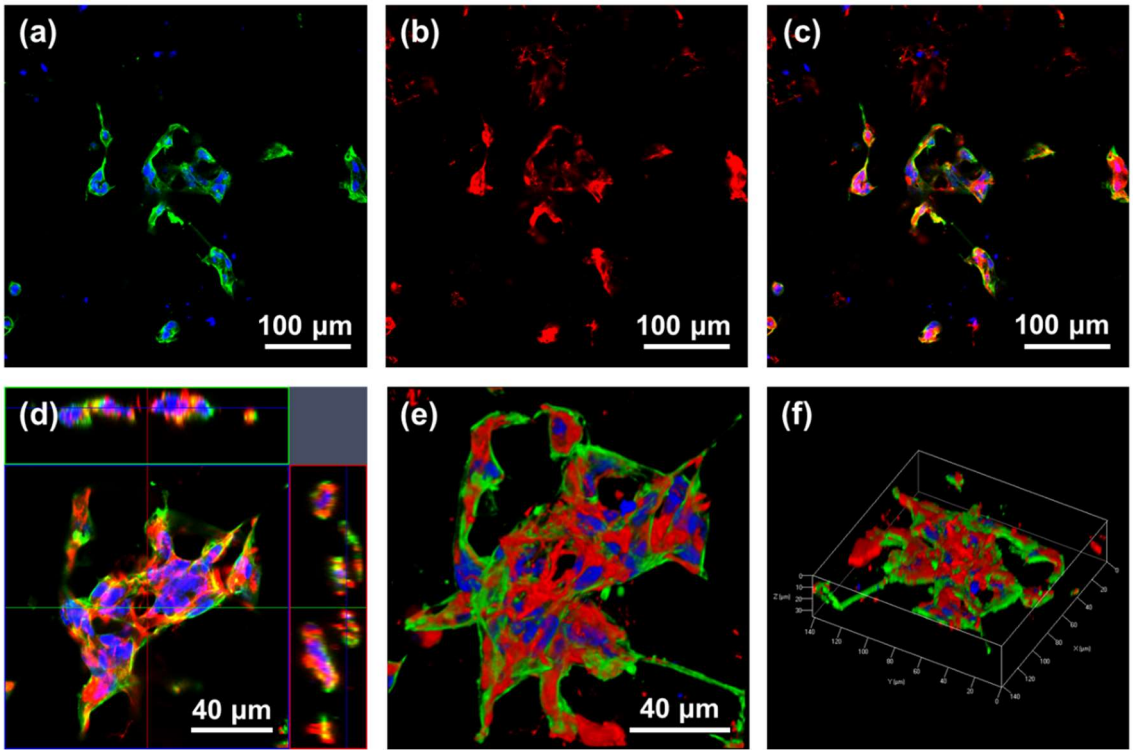

Figure 5.4 Immunofluorescence images of cell adhesion on control group scaffold. hMSCs were stained after cultured with osteogenic medium for 10 days. (Blue = nucleus, green = F-actin, red = collagen type I)

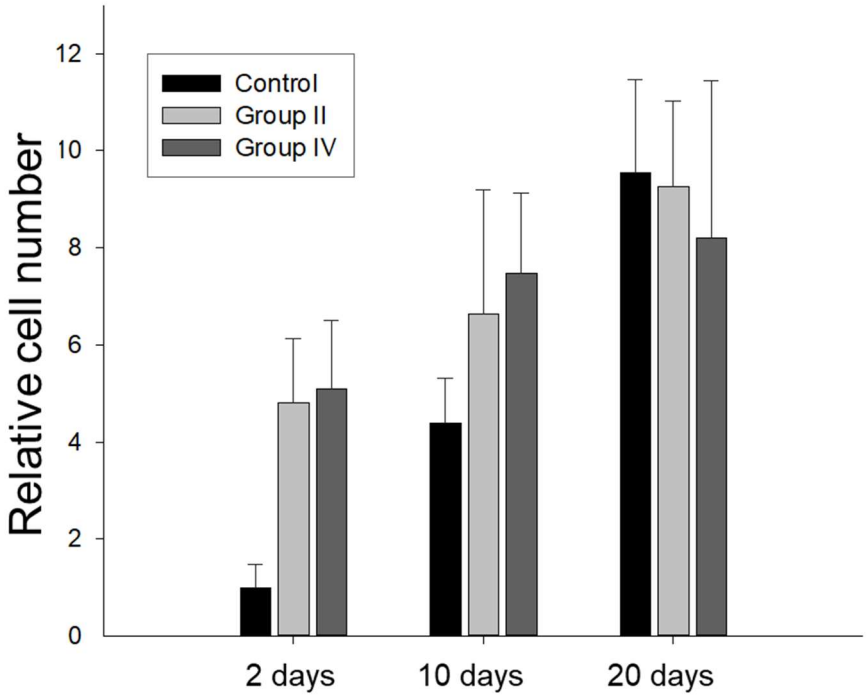

Figure 5.5 Proliferation assay result. All values were normalized to the absorbance of the control group measured after 2 days. (n=5)

5. Osteoinductivity of digested ECM in 3D

The osteoinductivity in each scaffold group was also confirmed by ARS staining. hMSCs were cultured on each group, control, II and IV for 10 days, then stained and washed until the dye residue was no longer dissolved out. The scaffold without cell was scarcely stained in all groups (fig. 6.1). The center and the boundary part of the scaffold were observed with a microscope. After 10 days, the control group was hardly stained, and the center of group II and group IV was stained with red color (fig. 6.2 (a) - (c)). At the boundary, the scaffold was stained along the outline of ECM fragment (fig. 6.2 (e) - (f)).

After staining, the amount of deposited mineral was quantified by cetylpyridinium chloride assay. In the w/o cell scaffolds, values were close to 0 in all groups, almost identical to the absorbance of only cetylpyridinium chloride solution. Group II and group IV showed a significant difference before and after culturing the cells and there was no significant difference between two groups after 10 days, although the mean value of group IV was slightly higher (fig. 6.3).

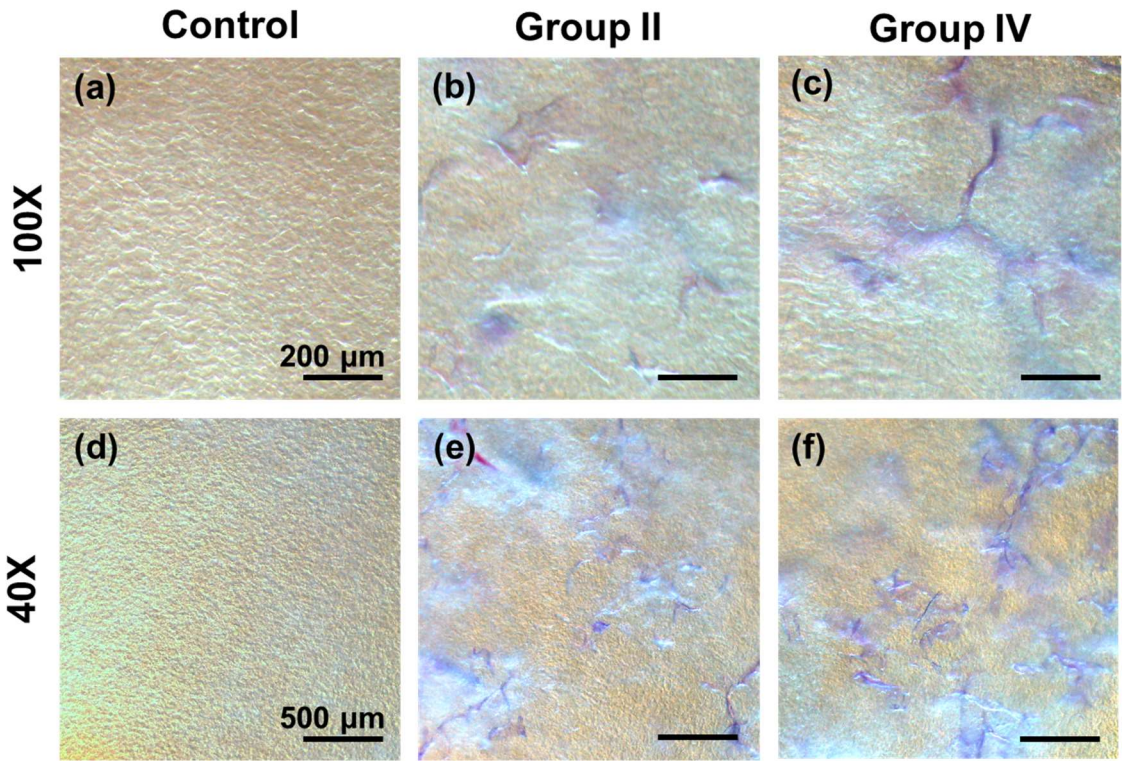

Figure 6.1 Alizarin red S staining results of the scaffolds. Scaffolds were stained right after manufactured, without cells.

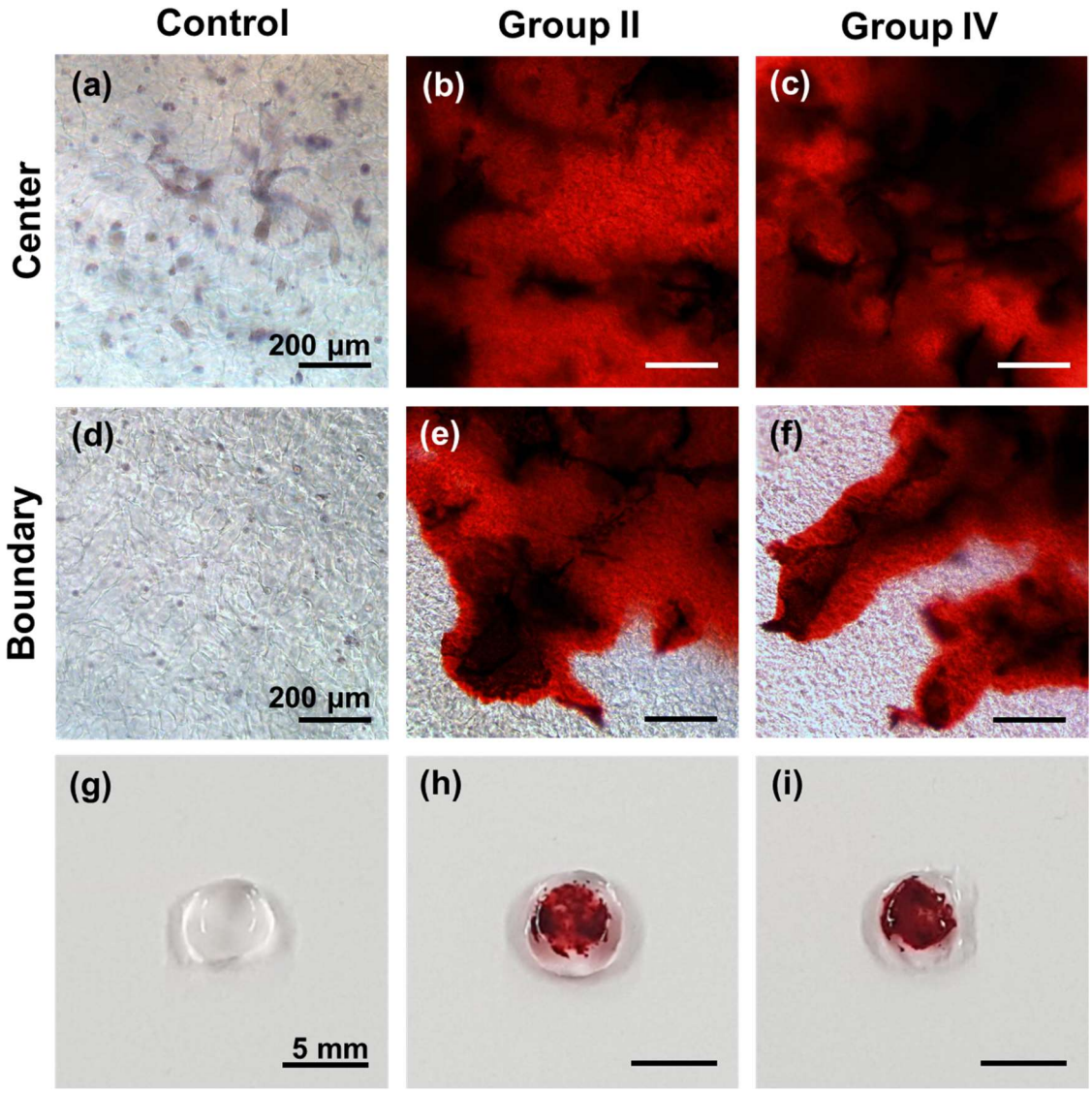

Figure 6.2 Alizarin red S staining results of the hMSCs cultured on the scaffolds. Scaffolds were stained after hMSCs were seeded and cultured with osteogenic medium for 10 days.

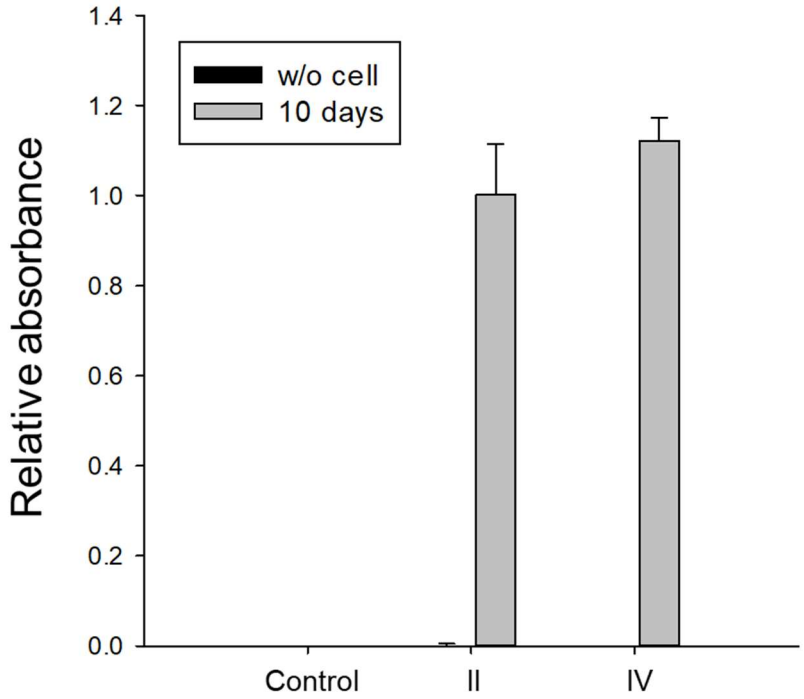

Figure 6.3 Quantification of deposited mineral on the scaffolds. Scaffolds were stained right after manufactured and 10 days after hMSCs cultured with osteogenic medium. All values were normalized with the absorbance value of only cetylpyridinium chloride 10% solution in DDW. (n=4)

Discussions

Conventional decellularization methods used to actual human or animal bones had to undergo several stages of processes and sterilization [4]. We designed a simpler process optimized for the ECM obtained in the laboratory. It is assumed that this method has advantage of proceeding in mild condition and fast than conventional methods. DAPI staining results showed that our decellularization process was sufficient from that no more blue dots were left.

We compared digested ECM with collagen type I at the 2D culture experiment. Because It is well known that major organic component of bone ECM is collagen type I [18], They had to be compared first in order to check whether the useful osteoinductive proteins were present in the ECM.

Alkaline phosphatase is the early osteogenic marker protein [19, 20]. Golub discovered that ALP activity is decreased as differentiation progress [21]. At the 20 days, however, digested ECM coated group rarely expressed ALP (fig. 2.1 (f)). In comparison with the photographs observed on the 10th day (fig. 2.1 (a) ~(c)) and the alizarin red S staining results, (fig. 2.2 A) the expression level of ALP was decreased as the osteogenesis progressed further. From these results, it was confirmed that digested ECM induced bone differentiation of hMSCs faster than other groups and preserved important osteoinductive agents distinct from collagen type I.

Mineralization is accompanied by proteins expressed in mature osteoblasts [22]. Therefore, it is possible to judge that the late osteogenic differentiation

progresses well through with the result of alizarin red S staining. ECM was demineralized through pepsin-HCl digestion process. Comparing (c) and (d) in the fig. 3.2, it can be seen that the stained mineral crystals were not originally present in the digested ECM but were newly deposited by stem cells. Therefore, the digested ECM coated group induced sufficient osteogenesis of hMSCs to have mineralization potential. And hMSCs cultured in digested ECM coated group mineralized significantly more than in other groups. With these staining results, we confirmed that the digested ECM induced specific and rapid differentiation of hMSCs into osteoblasts in 2D cell cultures.

PEGDA goes through radical polymerization with ammonium persulfate APS and TEMED. Ice crystals form between polymer network and construct porous structures [17]. Porous structure with regular pore size is important to hydrogel because it can affects scaffold's mechanical properties, cell adhesion and proliferation. Different cell interactions are promoted depending on the pore size of the scaffold, and the pore size suitable for bone regeneration and growth ranges from 40 to 400 μm [23]. Scaffolds that lost porous structure could greatly reduce the surface area of interaction with cells and lose their structural properties. The scaffolds were fabricated according to increasing digested ECM solution concentrations, and porous structure was observed through an electron microscope. Group I~IV, porous structure was well maintained in 40 ~ 400 μm scale and this result corresponded with fluorescence images of adhesion and distribution of cells (fig. 4.1 ~ 4.3).

Water absorbing ability is important property to hydrogel, including PEG scaffold. hydrogel's dynamics and chemical properties are completely changed depending on the presence of water. Young's modulus of the scaffold was measured in wet state, because after implantation scaffold would be in wet condition. The swelling ratio and young's modulus in these groups did not decrease much compared to the control, so it can be concluded that the modification of the PEG scaffold with digested ECM did not give a significant difference in mechanical properties. The Young's modulus needs to be similar to the actual bone for the scaffolds that replace bone itself [24], but scaffolds with lower young's modulus have the advantage that they can be applied to irregular bone defects. Also, PEG scaffolds can be made more rigid by increasing the molecular weight of PEG monomer, and can be slowly degraded and released to the outside of the body if manufactured with biodegradable crosslinkers.

PEG is very stable in the body and has the advantage of low foreign body reaction and protein adsorption, but it is difficult for cells to attach. So it's surface is usually modified by cell adhesion peptide like RGD or fibronectin [25]. Immunostaining result (fig. 4.1~4.4) and the low level of the control group in the CCK-8 assay result (fig. 4.5) suggest that the ECM improved the performance of the PEG scaffold by facilitating early cell adhesion. Since the absorbance increases in proportion to the number of living cells, the growth rate of the cells can be indirectly confirmed through CCK-8 assay. proliferation rate of cells slowed down at group II and IV, but as the stem cells differentiate, cells turn into

the G_0 phase of the cell division and decrease the proliferation rate [26]. With Alizarin red S staining and RT-PCR results, (fig. 5.2 ~ 5.4) the decrease in the rate of proliferation might be due to the progression of bone differentiation.

The results of Alizarin red S staining in the scaffold were similar to those in the 2D coating condition. Minerals were deposited specifically around the ECM fragment (fig. 5.2 (e), (f)). As a whole, it looks like the ECM on the outermost side of the scaffold formed borderline and the minerals were deposited among the ECM fragments. Scaffolds were totally minced with stainless spoon for extraction via cetylpyridinium chloride solution. Both group II and group IV scaffolds showed statistically significant higher amount of deposited mineral than control group scaffold. But there was no significant difference between group II and group IV. From this, it was confirmed that ECM fragments played an important role in mineralization. Mineralization occurs more rapidly in 3D than in 2D, which may be due to higher cell seeding concentrations or that 3D environment plays an important role in the maturation of osteoblasts [27].

Conclusions

ECM-cell complex produced from cell line in a lab could be much easily decellularized by simple steps, compared with general native tissue decellularization methods in previous works. Cell line-derived ECM induced osteogenesis of human mesenchymal stem cells. Even after decellularization and digestion, significant osteogenic factors in the ECM were preserved functionally. Cell line-derived ECM-hybrid scaffold was manufactured with appropriate ratio of components, resulting in well-constructed structure and pore size. Digested ECM enhanced cell adhesion and osteogenesis of hMSCs on the PEG scaffold when it was compared with control group. We concluded that cell line-derived ECM can be a new source of ECM used in tissue engineering instead of native ECM with this research.

References

[1] S.F. Badylak, The extracellular matrix as a scaffold for tissue reconstruction, Seminars in Cell & Developmental Biology 13(5) (2002) 377-383.

[2] S. Gronthos, K. Stewart, S.E. Graves, S. Hay, P.J. Simmons, Integrin expression and function on human osteoblast-like cells, Journal of Bone and Mineral Research 12(8) (1997) 1189-1197.

[3] D.M. Faulk, S.A. Johnson, L. Zhang, S.F. Badylak, Role of the extracellular matrix in whole organ engineering, Journal of Cellular Physiology 229(8) (2014) 984-989.

[4] P.M. Crapo, T.W. Gilbert, S.F. Badylak, An overview of tissue and whole organ decellularization processes, Biomaterials 32(12) (2011) 3233-3243.

[5] E. Gruskin, B.A. Doll, F.W. Futrell, J.P. Schmitz, J.O. Hollinger, Demineralized bone matrix in bone repair: history and use, Advanced Drug Delivery Reviews 64(12) (2012) 1063-1077.

[6] B. Peterson, P.G. Whang, R. Iglesias, J.C. Wang, J.R. Lieberman, Osteoinductivity of commercially available demineralized bone matrix, The Journal of Bone and Joint Surgery. American Volume 86-A(10) (2004) 2243-2250.

[7] B. Groessner-Schreiber, M. Krukowski, C. Lyons, P. Osdoby, Osteoclast recruitment in response to human bone matrix is age related, Mechanisms of Ageing and Development 62(2) (1992) 143-154.

[8] Z. Schwartz, A. Somers, J.T. Mellonig, D.L. Carnes, Jr., D.D. Dean, D.L. Cochran, B.D. Boyan, Ability of commercial demineralized freeze-dried bone

allograft to induce new bone formation is dependent on donor age but not gender, Journal of periodontology 69(4) (1998) 470-478.

[9] E. Munting, J.F. Wilmart, A. Wijne, P. Hennebert, C. Delloye, Effect of sterilization on osteoinduction. Comparison of five methods in demineralized rat bone, Acta orthopaedica Scandinavica 59(1) (1988) 34-38.

[10] J.L. Russell, J.E. Block, Clinical utility of demineralized bone matrix for osseous defects, arthrodesis, and reconstruction: impact of processing techniques and study methodology, Orthopedics 22(5) (1999) 524-31; quiz 532-533.

[11] E. Nyberg, A. Rindone, A. Dorafshar, W.L. Grayson, Comparison of 3D-Printed Poly-varepsilon-Caprolactone Scaffolds Functionalized with Tricalcium Phosphate, Hydroxyapatite, Bio-Oss, or Decellularized Bone Matrix, Tissue Engineering - Part A 23(11-12) (2017) 503-514.

[12] D. Wang, K. Christensen, K. Chawla, G. Xiao, P.H. Krebsbach, R.T. Franceschi, Isolation and characterization of MC3T3-E1 preosteoblast subclone with Distinct In Vitro and In Vivo Differentiation/Mineralization Potential, Journal of Bone and Mineral Research 14(6) (1999) 893-903.

[13] R.T. Franceschi, B.S. Iyer, Y. Cui, Effects of ascorbic acid on collagen matrix formation and osteoblast differentiation in murine MC3T3-E1 cells, Journal of Bone and Mineral Research 9(6) (1994) 843-854.

[14] C.R. Nuttelman, M.C. Tripodi, K.S. Anseth, Synthetic hydrogel niches that promote hMSC viability, Matrix Biology 24(3) (2005) 208-218.

[15] C.R. Nuttelman, M.A. Rice, A.E. Rydholm, C.N. Salinas, D.N. Shah, K.S. Anseth, Macromolecular Monomers for the Synthesis of Hydrogel Niches and Their Application in Cell Encapsulation and Tissue Engineering, Progress in polymer science 33(2) (2008) 167-179.

[16] D.O. Freytes, J. Martin, S.S. Velankar, A.S. Lee, S.F. Badylak, Preparation and rheological characterization of a gel form of the porcine urinary bladder matrix, Biomaterials 29(11) (2008) 1630-1637.

[17] Y. Hwang, N. Sangaj, S. Varghese, Interconnected macroporous poly(Ethylene Glycol) cryogels as a cell scaffold for cartilage tissue engineering, Tissue Engineering - Part A 16(10) (2010) 3033-3041.

[18] K. Anselme, Osteoblast adhesion on biomaterials, Biomaterials 21(7) (2000) 667-81.

[19] R.S. Siffert, The role of alkaline phosphatase in osteogenesis, The Journal of Experimental Medicine 93(5) (1951) 415.

[20] U. Stucki, J. Schmid, C.F. Hammerle, N.P. Lang, Temporal and local appearance of alkaline phosphatase activity in early stages of guided bone regeneration. A descriptive histochemical study in humans, Clinical Oral Implants Research 12(2) (2001) 121-127.

[21] E.E. Golub, K. Boesze-Battaglia, The role of alkaline phosphatase in mineralization, Current Opinion in Orthopaedics 18(5) (2007) 444-448.

[22] A.C. Allori, A.M. Sailon, S.M. Warren, Biological basis of bone formation, remodeling, and repair-part II: extracellular matrix, Tissue Engineering - Part B:

Reviews 14(3) (2008) 275-283.

[23] F.J. O'Brien, B.A. Harley, I.V. Yannas, L.J. Gibson, The effect of pore size on cell adhesion in collagen-GAG scaffolds, Biomaterials 26(4) (2005) 433-441.

[24] M. Niinomi, Y. Liu, M. Nakai, H. Liu, H. Li, Biomedical titanium alloys with Young's moduli close to that of cortical bone, Regenerative Biomaterials 3(3) (2016) 173-185.

[25] J. Zhu, Bioactive modification of poly(ethylene glycol) hydrogels for tissue engineering, Biomaterials 31(17) (2010) 4639-4656.

[26] J.P. Matson, J.G. Cook, Cell cycle proliferation decisions: the impact of single cell analyses, The FEBS Journal 284(3) (2017) 362-375.

[27] S. Kale, S. Biermann, C. Edwards, C. Tarnowski, M. Morris, M.W. Long, Three-dimensional cellular development is essential for ex vivo formation of human bone, Nature Biotechnology 18(9) (2000) 954-958.

요약 (국문초록)

MC3T3-E1 세포주 유래 세포외기질과 융합된 PEG 3차원 지지체의 골분화능

세포외기질은 조직의 세포들 사이를 메꾸고 있는 세포들이 분비한 물질로, 생체 내의 미소 환경을 보존하고 있다. 줄기세포의 분화와 성장, 부착 등에 영향을 줄 수 있음이 밝혀져 조직공학 분야에서 최근 활발히 연구되고 있다. 기존의 ECM을 활용하는 연구는 인간이나 돼지, 소의 장기를 대상으로 진행되었는데, 공급이 제한적이고 개체의 건강 상태나 연령 등 여러 요소에 따라 ECM의 조성이나 효능이 달라지며, 동종 및 이종 간의 전염병을 옮길 수 있다는 한계를 가진다. 이에 비하여 실험실에서 배양한 세포주로부터 얻어지는 세포외기질은 균일한 품질로 통제된 환경 하에서 생산될 수 있다는 장점을 가진다. 본 연구팀은 이에 착안해 뼈 세포주 MC3T3-E1의 세포외기질에서 세포들을 제거하는 최적화된 공정을 설계하고, 이를 가수분해한 후 인간 중간엽 줄기세포를 배양하여 골 분화능을 평가하였다. 2차원에서 세포배양접시를 코팅한 것과 PEG 3차원 지지체에 ECM을 융합한 세포배양조건 모두에서 골분화가 유도되었음을 확인했다. 이번 연구는 세포주에서 유래한 세포외기질의 조직공학 분야에서의 활용 가능성을 제시한다는 의의를 가진다.

주요어 : 골분화, 중간엽줄기세포, 세포외기질, 뼈재생, 조직공학, PEG, 스캐폴드

학 번 : 2016-21013